Scintillation Properties of Eu-doped KI Single Crystals

Keiichiro Miyazaki,* Daisuke Nakauchi, Takumi Kato,
Noriaki Kawaguchi, and Takayuki Yanagida

Division of Materials Science, Nara Institute of Science and Technology,
8916-5 Takayama-cho, Ikoma-shi, Nara 630-0192, Japan

The photoluminescence and scintillation properties of KI:Eu synthesized by the vertical Bridgman–Stockbarger method were investigated. All the samples showed a broad peak at 430–450 nm under UV and X-ray irradiations, and the origin of emission was ascribed to the $4f^6 5d^1$–$4f^7$ transition of Eu^{2+}. Furthermore, a tail emission at 500 nm under X-ray irradiation was observed, the origin of which could be ascribed to color centers associated with oxygen impurities. According to the pulse height spectra, the highest light yield (*LY*) under ^{241}Am γ-ray (60 keV) irradiation was 3400 photons/MeV among the prepared samples. In terms of *LY* and afterglow, the optimal concentration of Eu was found to be 0.3%.

1. Introduction

Scintillators are phosphors that convert ionizing radiation to numerous low-energy photons in the range of ultraviolet (UV) to near-infrared (NIR) light. By combining scintillators and photodetectors such as photomultiplier tubes (PMTs) and photodiodes (PDs), ionizing radiation can be detected as an electrical signal.[1] Therefore, scintillators have been used in radiation measurement fields such as medicine,[2] environmental measurement,[3,4] well logging,[5] and security.[6] The following properties of X- and γ-ray scintillators are required: high light yield (*LY*), high energy resolution, large effective atomic number (Z_{eff}), short decay time, low afterglow, and no hygroscopicity. There are no scintillators that meet all the required properties, and material exploration continues at present. So far, material forms such as glass,[7–16] ceramics,[17–26] and single crystals[27–36] have been developed. Among the material forms, single crystals have mainly been studied because of their high luminescence intensity.

While most halide materials are hygroscopic,[37] some of them have been used in practice owing to their high *LY*.[38] In addition, the manufacturing cost of these materials is low because the melting point is relatively low. The typical halide scintillators, NaI:Tl and CsI:Tl, show high *LY* and energy resolution, and the emission wavelengths of NaI:Tl and CsI:Tl are suitable for PMTs and PDs, respectively.[39,40] Since dopant-activated NaI and CsI have been widely used for a long time, other alkali iodides are also high-potential scintillator hosts. In our previous study,

---

the scintillation properties of KI:Tl and RbI:Tl were investigated because they have less hygroscopicity than NaI,[41,42] and KI:Tl showed a moderate *LY* of 7300 photons/MeV. In addition to Tl-doped ones, Eu-doped alkali iodides such as LiI:Eu, NaI:Eu, and CsI:Eu have also been reported to show a high *LY* of 15000–20000 photons/MeV;[43–45] therefore, KI:Eu would be expected to show a high *LY*. So far, there have been a few reports on the photoluminescence (PL) of KI:Eu.[46] However, no reports on the scintillation properties of KI:Eu exist. In this study, KI:Eu single crystals were grown by the vertical Bridgman–Stockbarger method, and the concentration dependences of Eu on photoluminescence and scintillation properties were evaluated.

2.   Experimental Methods

Undoped KI and KI:Eu single crystals were synthesized by the vertical Bridgman–Stockbarger method, and the concentrations of Eu were 0.03, 0.1, 0.3, and 1%. KI (High Purity Chemicals, 2N) and EuI_2 (Sigma Aldrich, 5N) were mixed in stoichiometric ratio in a glove box (AZGBV065, Glovebox Japan inc.). These powders were put into a quartz tube and dried by heating at 200 ºC for 2 h in vacuum. Then, the quartz tube was sealed using a gas burner[47,48] and set in a Bridgman furnace (VFK-1800, Crystal Systems). The temperature of the furnace was 730 ºC, which was ~50 ºC above the melting point of KI,[49] and the pull-down speed was 5 mm/h. After growth, the quartz tubes were crushed to obtain samples with the size of ~5 mmϕ × 10–20 mm. The two large surfaces were polished using sandpaper. In the case of PL properties, PL contour plots and quantum yields (*QY*s) were obtained using Quantaurus-QY (C11347, Hamamatsu Photonics). PL decay curves were measured using Quantaurus-τ (C11367, Hamamatsu Photonics). X-ray-induced scintillation spectra were measured using our original setup.[50] The applied voltage and current of the X-ray tube were 60 kV and 1.2 mA, respectively. X-ray-induced scintillation decay curves and afterglow profiles were obtained using an X-ray-induced afterglow characterization system.[51] To estimate *LY*, pulse height spectra were measured using PMT (R7600U-200, Hamamatsu Photonics) and a ^{241}Am γ-ray source.

3.   Results and Discussion

Pictures of the samples under room light and UV light irradiation are shown in Fig. 1. The thickness of all the samples was unified as 1–2 mm. All the samples were colorless and transparent under room light, and all the samples showed blue emission under 365 nm UV irradiation. The PL contour plots of all the samples are illustrated in Fig. 2. All the samples showed an emission peak at 430–450 nm under excitation at 300–400 nm. The emission wavelength was shifted toward long wavelengths with increasing Eu concentration, and the values of the Stokes shift in the 0.03, 0.1, 0.3, and 1% Eu-doped samples under 390 nm irradiation were 45.1, 48.1, 51.9, and 52.6 nm, respectively. The *QY*s of the 0.03, 0.1, 0.3, and 1% Eu-doped samples under excitation at 360 nm were >99, >99, 97, and 96%, respectively. The PL decay time curves monitored at 440 nm under excitation at 365 nm are shown in Fig. 3. All the decay curves were composed of one exponential function, and the decay time constant (τ) was 1.18–1.49 ms.
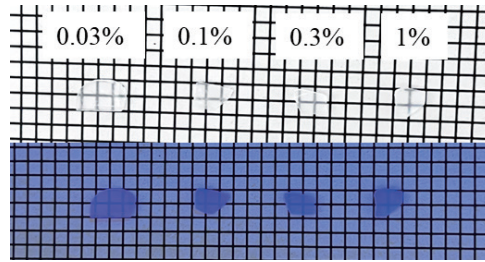
Fig. 1. (Color online) Pictures of crystalline KI doped with various concentrations of Eu (0.03, 0.1, 0.3, and 1%) under room light (top) and UV light at 365 nm (bottom).
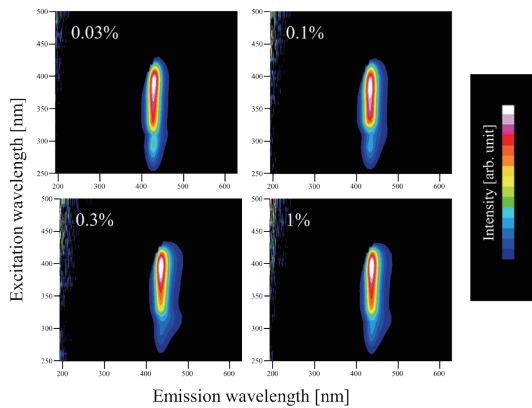

Fig. 2. (Color online) PL contour plots of KI:Eu. The vertical and horizontal axes are emission and excitation wavelengths, respectively.
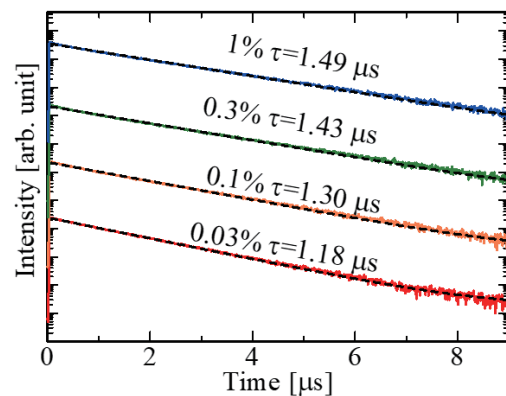

Fig. 3. (Color online) PL decay curves monitored at 440 nm under 365 nm excitation. Dashed lines are fitting curves.

This emission would be ascribed to the $4f^65d^1$–$4f^7$ transition of Eu^{2+} because the emission wavelength and PL decay time constant were close to those of KI:Eu.[46,52]

The X-ray-induced scintillation spectra of KI:Eu and an undoped KI are presented in Fig. 4. A broad peak at 430–450 nm was observed, and this peak would be ascribed to the $4f^65d^1$–$4f^7$ transition of Eu^{2+} since the emission wavelength was close to PL (Fig. 2). The peak shift was observed as well as PL in Fig. 2. In addition, a tail emission was observed at ~500 nm. In the undoped KI, the emission signals were observed at around 300, 400, and 500 nm. According to previous reports,[53,54] the emissions at 300 and 400 nm were on- and off-center configurations of self-trapped excitons, respectively, and the luminescence at 500 nm was ascribed to color centers associated with oxygen impurities.[55] Scintillation decay curves under X-ray irradiation in KI:Eu are indicated in Fig. 5. All the decay profiles consisted of a sum of two exponential functions. Here, the fast and slow components were indicated as τ_1 and τ_2, respectively. Because τ_1 was close to the PL decay time constant, τ_1 would be attributed to the $4f^65d^1$–$4f^7$ transition of Eu^{2+}. The τ_2 would be color centers associated with oxygen impurities. In some materials, the high excitation density of X-ray irradiation generates many secondary electrons, and the interaction between many localized secondary electrons causes quenching.[56–60] Such quenching makes the scintillation decay time constants shorter than those of PL decays.
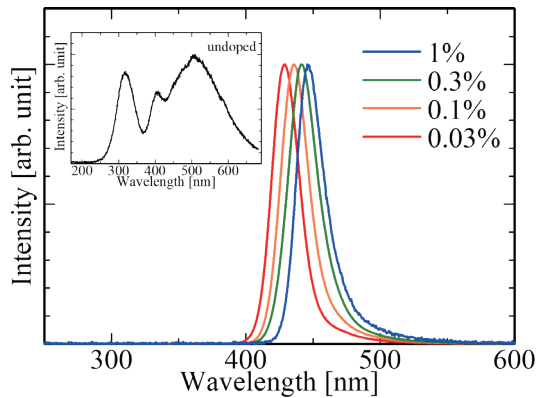
Fig. 4.   (Color online) X-ray-induced scintillation spectra of KI:Eu and undoped KI (inset).
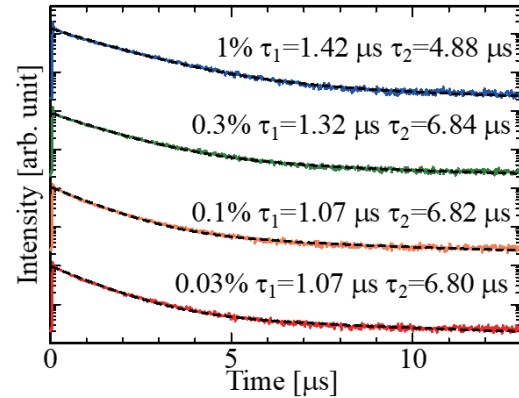

Fig. 5.   (Color online) X-ray-induced scintillation decay profiles of KI:Eu. Dashed lines are fitting curves.

Afterglow profiles after X-ray exposure for 2 ms in KI:Eu are shown in Fig. 6. Here, the afterglow levels at 20 ms after the X-ray was turned off were defined using the following equation: Afterglow level [ppm] = $10^6 \times (I_2 - I_{BG})/(I_1 - I_{BG})$,[61,62] where I_1 is the signal intensity during X-ray irradiation, I_2 is the signal intensity at 20 ms after the X-ray is turned off, and I_{BG} is the background signal intensity. The afterglow levels of the 0.03, 0.1, 0.3, and 1% Eu-doped samples were 1600, 1200, 700, and 9500 ppm, respectively. The 0.3% Eu-doped sample showed the lowest afterglow level among all the samples. In the 0.03, 0.1, and 0.3% Eu-doped samples, Eu^{2+} would be substituted at the K^+ site. However, excess Eu^{2+} might distort the crystal structure in the 1% Eu-doped sample. Such a lattice distortion can lead to the generation of defects, and the afterglow level of the 1% Eu-doped sample can become high.

Pulse height spectra measured using KI:Eu and reference Gd_2SiO_5:Ce (GSO:Ce) under ^{241}Am γ-ray (60 keV) irradiation are presented in Fig. 7. The shaping times of KI:Eu and GSO:Ce were 3 and 0.5 ms, respectively. The *LY* of GSO:Ce was reported to be 8000 photons/MeV,[63–65] and the peak channel was directly compared with the calculated *LY* since the wavelengths of KI:Eu and GSO:Ce were almost the same. Concerning the signals due to the Compton edge, the photoabsorption peaks of low-energy γ-rays and 60 keV were overlapped in the 0.03 and 0.1% Eu-doped samples, and a photoabsorption peak was observed at ~200 ch in the 0.3 and 1% Eu-doped samples. The *LY*s of the 0.3 and 1% Eu-doped samples were 3400 and 3300 photons/MeV, respectively. Since the measured value contained a 10% error, the *LY*s of the 0.3 and 1% Eu-doped samples were not significantly different. The scintillation *LY* can be expressed using the following equation: $LY \propto S \times QY$, where S is the energy transportation efficiency from a host to a luminescence center.[66] The PL *QY* of all the samples was >96%. Therefore, energy transportation would be inefficient. Scintillation *LY*s have been reported to be inversely correlated with storage-type luminescence, such as thermoluminescence and optically stimulated luminescence.[67] In this study, the afterglow did not correlate with the scintillation *LY* probably because the afterglow did not include storage luminescence but only thermoluminescence at room temperature.
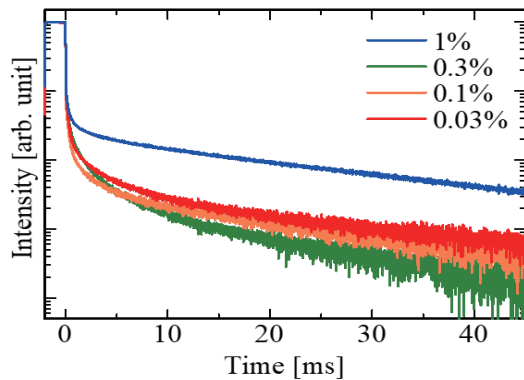
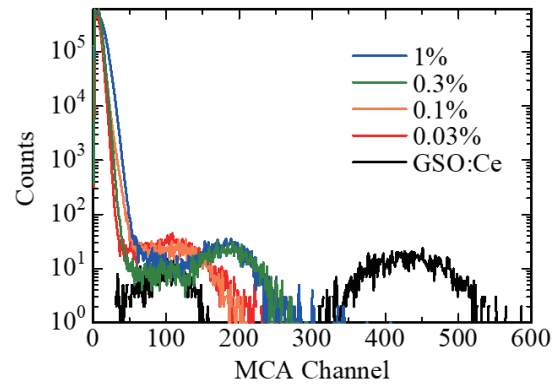Fig. 6.   (Color online) Afterglow profiles after X-ray exposure for 2 ms.

Fig. 7.   (Color online) Pulse height spectra of KI:Eu and Gd_2SiO_5:Ce (GSO:Ce) under ^{241}Am γ-ray (60 keV) irradiation.

4.   Conclusions

The photoluminescence and scintillation properties of KI:Eu synthesized by the vertical Bridgman–Stockbarger method were investigated. A broad peak due to the $4f^65d^1$–$4f^7$ transition of Eu^{2+} was observed at 430–450 nm under UV and X-ray irradiations. In addition, a tail emission ascribed to color centers associated with oxygen impurities was observed at 500 nm under X-ray irradiation. According to the pulse height spectra under ^{241}Am γ-ray (60 keV) irradiation, the highest *LY* was 3400 photons/MeV among the prepared samples. In terms of *LY* and afterglow, the optimal concentration of Eu was 0.3% in KI. However, KI:Eu showed a lower *LY* than commercial scintillators, and the energy transportation would be inefficient. Therefore, the *LY* can be improved if the synthesis conditions are optimized to decrease the number of defects.

References

1   T. Yanagida: Proc. Jpn. Acad. Ser. B **94** (2018) 75. https://doi.org/10.2183/pjab.94.007
2   V. Babin, V. V. Laguta, M. Nikl, J. Pejchal, A. Yoshikawa, and S. Zazubovich: Opt. Mater. **103** (2020) 109832. https://doi.org/10.1016/j.optmat.2020.109832
3   S. Yamamoto and H. Tomita: Appl. Radiat. Isot. **168** (2021) 109527. https://doi.org/10.1016/j.apradiso.2020.109527

4   G. Tanaka and H. Kawamura: J. Radiat. Res. **19** (1978) 78. https://doi.org/10.1269/jrr.19.78
5   M. J. Weber and R. R. Monchamp: J. Appl. Phys. **44** (1973) 5495. https://doi.org/10.1063/1.1662183
6   V. D. Ryzhikov, A. D. Opolonin, P. V. Pashko, V. M. Svishch, V. G. Volkov, E. K. Lysetskaya, D. N. Kozin, and C. Smith: Nucl. Instrum. Methods Phys. Res., Sect. A **537** (2005) 424. https://doi.org/10.1016/j.nima.2004.08.056
7   N. Kawaguchi, K. Watanabe, D. Shiratori, T. Kato, D. Nakauchi, and T. Yanagida: Sens. Mater. **35** (2023) 499. https://doi.org/10.18494/SAM4136
8   Y. Takebuchi, D. Shiratori, T. Kato, D. Nakauchi, N. Kawaguchi, and T. Yanagida: Sens. Mater. **35** (2023) 507. https://doi.org/10.18494/SAM4142
9   H. Fukushima, D. Shiratori, D. Nakauchi, T. Kato, N. Kawaguchi, and T. Yanagida: Sens. Mater. **34** (2022) 717. https://doi.org/10.18494/SAM3691
10 R. Nakamori, N. Kawano, A. Takaku, D. Onoda, Y. Takebuchi, H. Fukushima, T. Kato, K. Shinozaki, and T. Yanagida: Sens. Mater. **34** (2022) 707. https://doi.org/10.18494/SAM3689
11 H. Kimura, T. Fujiwara, M. Tanaka, T. Kato, D. Nakauchi, N. Kawaguchi, and T. Yanagida: Sens. Mater. **35** (2023) 513. https://doi.org/10.18494/SAM4146
12 H. Masai and T. Yanagida: Jpn. J. Appl. Phys. **62** (2023) 010606. https://doi.org/10.35848/1347-4065/ac91b8
13 N. Wantana, E. Kaewnuam, Y. Tariwong, N. D. Quang, P. Pakawanit, C. Phoovasawat, N. Vittayakorn, S. Kothan, H. J. Kim, and J. Kaewkhao: Jpn. J. Appl. Phys. **62** (2023) 010602. https://doi.org/10.35848/1347-4065/ac9876
14 A. Nishikawa, D. Shiratori, T. Kato, D. Nakauchi, N. Kawaguchi, and T. Yanagida: Ceram. Int. **50** (2024) 3772. https://doi.org/10.1016/j.ceramint.2023.11.130
15 H. Kimura, K. Shinozaki, G. Okada, N. Kawaguchi, and T. Yanagida: J. Non-Cryst. Solids **508** (2019) 46. https://doi.org/10.1016/j.jnoncrysol.2018.11.020
16 Y. Nakabayashi, Y. Fujimoto, M. Koshimizu, and K. Asai: Opt. Mater. **142** (2023) 114136. https://doi.org/10.1016/j.optmat.2023.114136
17 Y. Yoshikawa, T. Kato, D. Nakauchi, N. Kawaguchi, and T. Yanagida: Radiat. Phys. Chem. **215** (2024) 111367. https://doi.org/10.1016/j.radphyschem.2023.111367
18 D. Nakauchi, F. Nakamura, T. Kato, N. Kawaguchi, and T. Yanagida: Sens. Mater. **35** (2023) 467. https://doi.org/10.18494/SAM4138
19 T. Kunikata, T. Kato, D. Shiratori, P. Kantuptim, D. Nakauchi, N. Kawaguchi, and T. Yanagida: Sens. Mater. **35** (2023) 491. https://doi.org/10.18494/SAM4145
20 T. Kunikata, T. Kato, D. Shiratori, D. Nakauchi, N. Kawaguchi, and T. Yanagida: Sens. Mater. **34** (2022) 661. https://doi.org/10.18494/SAM3683
21 Y. Shao, R. L. Conner, N. R. S. Souza, R. S. Silva, and L. G. Jacobsohn: Jpn. J. Appl. Phys. **62** (2023) 010601. https://doi.org/10.35848/1347-4065/ac9941
22 T. Yanagida, H. Takahashi, T. Ito, D. Kasama, T. Enoto, M. Sato, S. Hirakuri, M. Kokubun, K. Makishima, T. Yanagitani, H. Yagi, T. Shigeta, and T. Ito: IEEE Trans. Nucl. Sci. **52** (2005) 1836. https://doi.org/10.1109/TNS.2005.856757
23 S. Otake, H. Sakaguchi, Y. Yoshikawa, T. Kato, D. Nakauchi, N. Kawaguchi, and T. Yanagida: Radiat. Meas. **169** (2023) 107032. https://doi.org/10.1016/j.radmeas.2023.107032
24 H. Kimura, T. Kato, D. Nakauchi, G. Okada, N. Kawaguchi, and T. Yanagida: Nucl. Instrum. Methods Phys. Res. Sect. A **954** (2020) 161226. https://doi.org/10.1016/j.nima.2018.09.061
25 Y. Yoshikawa, T. Kato, D. Nakauchi, N. Kawaguchi, and T. Yanagida: Jpn. J. Appl. Phys. **61** (2022) 102001. https://doi.org/10.35848/1347-4065/ac88ab
26 Y. Yoshikawa, T. Kato, K. Miyazaki, D. Nakauchi, N. Kawaguchi, and T. Yanagida: Nucl. Instrum. Methods Phys. Res., Sect. B **546** (2024) 165155. https://doi.org/10.1016/j.nimb.2023.165155
27 H. Fukushima, D. Nakauchi, T. Kato, N. Kawaguchi, and T. Yanagida: Sens. Mater. **35** (2023) 429. https://doi.org/10.18494/SAM4139
28 D. Shiratori, H. Fukushima, D. Nakauchi, T. Kato, N. Kawaguchi, and T. Yanagida: Sens. Mater. **35** (2023) 439. https://doi.org/10.18494/SAM4140
29 K. Okazaki, D. Nakauchi, H. Fukushima, T. Kato, N. Kawaguchi, and T. Yanagida: Sens. Mater. **35** (2023) 459. https://doi.org/10.18494/SAM4144
30 T. Yanagida, T. Kato, D. Nakauchi, and N. Kawaguchi: Sens. Mater. **34** (2022) 595. https://doi.org/10.18494/SAM3684
31 P. Kantuptim, D. Nakauchi, T. Kato, N. Kawaguchi, and T. Yanagida: Sens. Mater. **34** (2022) 603. https://doi.org/10.18494/SAM3690

32   D. Nakauchi, H. Fukushima, T. Kato, N. Kawaguchi, and T. Yanagida: Sens. Mater. **34** (2022) 611. https://doi.org/10.18494/SAM3696

33   M. Akatsuka, N. Daisuke, K. Takumi, N. Kawaguchi, and T. Yanagida: Sens. Mater. **34** (2022) 619. https://doi.org/10.18494/SAM3692

34   Y. Fujimoto, D. Nakauchi, T. Yanagida, M. Koshimizu, and K. Asai: Sens. Mater. **34** (2022) 629. https://doi.org/10.18494/SAM3693

35   P. Kantuptim, T. Kato, D. Nakauchi, N. Kawaguchi, K. Watanabe, and T. Yanagida: Sens. Mater. **35** (2023) 451. https://doi.org/10.18494/SAM4141

36   H. Fukushima, D. Nakauchi, N. Kawaguchi, and T. Yanagida: Jpn. J. Appl. Phys. **58** (2019) 052005. https://doi.org/10.7567/1347-4065/ab116c

37   M. Zhuravleva, L. Stand, H. Wei, C. Hobbs, L. A. Boatner, J. O. Ramey, K. Shah, A. Burger, E. Rowe, P. Bhattacharya, E. Tupitsyn, and C. L. Melcher: 2013 IEEE Nucl. Sci. Symp. Med. Imaging Conf. (2013 NSS/MIC) (2013) 1. https://doi.org/10.1109/NSSMIC.2013.6829669

38   P. Dorenbos: Opt. Mater.: X **1** (2019) 100021. https://doi.org/10.1016/j.omx.2019.100021

39   I. V. Khodyuk, P. A. Rodnyi, and P. Dorenbos: J. Appl. Phys. **107** (2010) 113513. https://doi.org/10.1063/1.3431009

40   B. K. Cha, J. H. Shin, J. H. Bae, C. hun Lee, S. Chang, H. K. Kim, C. K. Kim, and G. Cho: Nucl. Instrum. Methods Phys. Res., Sect. A **604** (2009) 224. https://doi.org/10.1016/j.nima.2009.01.177

41   K. Miyazaki, D. Nakauchi, T. Kato, N. Kawaguchi, and T. Yanagida: J. Mater. Sci. Mater. Electron. **33** (2022) 22162. https://doi.org/10.1007/s10854-022-08996-y

42   K. Miyazaki, D. Nakauchi, T. Kato, N. Kawaguchi, and T. Yanagida: Radiat. Phys. Chem. (2023) 110820. https://doi.org/10.1016/j.radphyschem.2023.110820.

43   A. Syntfeld, M. Moszyński, R. Arlt, M. Balcerzyk, M. Kapusta, M. Majorov, R. Marcinkowski, P. Schotanus, M. Swoboda, and D. Wolski: IEEE Trans. Nucl. Sci. **52** (2005) 3151. https://doi.org/10.1109/TNS.2005.860193

44   I. Holl, E. Lorenz, and G. Mageras: IEEE Trans. Nucl. Sci. **35** (1988) 105. https://doi.org/10.1109/23.12684

45   N. V. Shiran, A. V. Gektin, Y. Boyarintseva, S. Vasyukov, A. Boyarintsev, V. Pedash, S. Tkachenko, O. Zelenskaya, N. Kosinov, O. Kisil, and L. Philippovich: IEEE Trans. Nucl. Sci. **57** (2010) 1233. https://doi.org/10.1109/TNS.2010.2048578

46   J. Rubio O: J. Phys. Chem. Solids **52** (1991) 101. https://doi.org/10.1016/0022-3697(91)90062-5

47   D. Nakauchi, Y. Fujimoto, T. Kato, N. Kawaguchi, and T. Yanagida: Jpn. J. Appl. Phys. **60** (2021) 2. https://doi.org/10.35848/1347-4065/ac15af

48   G. Ito, H. Kimura, D. Shiratori, D. Nakauchi, T. Kato, N. Kawaguchi, and T. Yanagida: Sens. Mater. **34** (2022) 685. https://doi.org/10.18494/SAM3681

49   I. Klavina, T. Kaljuvee, K. Timmo, J. Raudoja, R. Traksmaa, M. Altosaar, and D. Meissner: Thin Solid Films **519** (2011) 7399. https://doi.org/10.1016/j.tsf.2011.01.365

50   T. Yanagida, K. Kamada, Y. Fujimoto, H. Yagi, and T. Yanagitani: Opt. Mater. **35** (2013) 2480. https://doi.org/10.1016/j.optmat.2013.07.002

51   T. Yanagida, Y. Fujimoto, T. Ito, K. Uchiyama, and K. Mori: Appl. Phys. Express **7** (2014) 4. https://doi.org/10.7567/APEX.7.062401

52   R. Pérez-Salas, T. M. Piters, R. Aceves, R. Rodríguez-Mijangos, H. Riveros, J. M. Hernández A., and H. Murrieta S.: Opt. Mater. **35** (2013) 617. https://doi.org/10.1016/j.optmat.2012.10.016

53   K. Shunkeyev, L. Myasnikova, A. Barmina, and S. Sagimbaeva: J. Phys. Conf. Ser. **400** (2012) 042002. https://doi.org/10.1088/1742-6596/400/4/042002

54   R. T. Williams and K. S. Song: J. Phys. Chem. Solids **51** (1990) 679. https://doi.org/10.1016/0022-3697(90)90144-5

55   R. Fieschi and G. Spinolo: Nuovo Cim. **23** (1962) 738. https://doi.org/10.1007/BF02732742

56   R. Nakamori, N. Kawano, A. Takaku, D. Nakauchi, H. Kimura, M. Akatsuka, K. Shinozaki, and T. Yanagida: Mater. Res. Bull. **145** (2022) 111547. https://doi.org/10.1016/j.materresbull.2021.111547

57   K. Shinozaki, Y. Fujimoto, G. Okada, N. Kawaguchi, T. Yanagida, and T. Akai: J. Mater. Sci. Mater. Electron. **29** (2018) 11824. https://doi.org/10.1007/s10854-018-9282-y

58   D. Nakauchi, G. Okada, N. Kawano, N. Kawaguchi, and T. Yanagida: Appl. Phys. Express **10** (2017) 072601. https://doi.org/10.7567/APEX.10.072601

59   T. Yanagida and G. Okada: J. Ceram. Soc. Jpn. **124** (2016) 564. https://doi.org/10.2109/jcersj2.15237

60   G. Okada, T. Kojima, J. Ushizawa, N. Kawaguchi, and T. Yanagida: Curr. Appl. Phys. **17** (2017) 422. https://doi.org/10.1016/j.cap.2017.01.004

61   D. Nakauchi, T. Kato, N. Kawaguchi, and T. Yanagida: Appl. Phys. Express **13** (2020) 2. https://doi.org/10.35848/1882-0786/abc574

62   K. Miyazaki, D. Nakauchi, T. Kato, N. Kawaguchi, and T. Yanagida: J. Mater. Sci. Mater. Electron. **34** (2023) 4. https://doi.org/10.1007/s10854-023-10517-4

63   I. G. Valais, I. S. Kandarakis, D. N. Nikolopoulos, C. M. Michail, S. L. David, G. K. Loudos, D. A. Cavouras, and G. S. Panayiotakis: IEEE Trans. Nucl. Sci. **54** (2007) 11. https://doi.org/10.1109/TNS.2006.888813

64   I. Valais, C. Michail, S. David, C. D. Nomicos, G. S. Panayiotakis, and I. Kandarakis: Physica Med. **24** (2008) 122. https://doi.org/10.1016/j.ejmp.2008.01.007

65   Y. Fujimoto, D. Nakauchi, T. Yanagida, M. Koshimizu, and K. Asai: Sens. Mater. **33** (2021) 2147. https://doi.org/10.18494/SAM.2021.3321

66   D. J. Robbins: J. Electrochem. Soc. **127** (1980) 2694. https://doi.org/10.1149/1.2129574

67   T. Yanagida: J. Lumin. **169** (2016) 544. https://doi.org/10.1016/j.jlumin.2015.01.006